ARCHIVES OF TRANSPORT *ISSN (print):* *0866-9546*
Volume 62, Issue 2, 2022 ***e-ISSN (online):*** *2300-8830*
DOI: *10.5604/01.3001.0015.9253*

SATURATED ARTERIAL COORDINATE CONTROL STRATEGY OPTIMIZATION CONSIDERING MACROSCOPIC FUNDAMENTAL DIAGRAM

Xuanhua LIN[1], Xiaohui LIN[2], Kelian CHEN[3]

[1, 2, 3] Institute of Rail Traffic, Guangdong Communication Polytechnic, Guangzhou, China

Abstract*:*

MFD is widely used in traffic state evaluation because of its description of the macro level of urban road network. Aiming at the control strategy optimization problem of urban arterial road network under saturated traffic flow state, this study analyzes the MFD characteristics of a typical three-segment "ascending-stable-descending segment" and its advantages in characterizing the macroscopic operation efficiency of the road network, a arterial coordination control strategy considering MFD is proposed. According to the characteristics of MFD, it is proposed that the slope of the ascending segment and the capacity of the road network represent the operating efficiency of the free flow and saturated flow of the road network respectively. The traffic flow and density data of road segment are obtained by the road detector through Vissim simulation software. Aiming at the problem that the MFD is too discrete due to unreasonable control strategy or traffic condition, and in order to extract the MFD optimization target indicators, it is proposed to extract the key boundary points of the MFD by the "tic-tac-toe" method and divide the MFD state by Gaussian mixture clustering. The genetic algorithm integrates the multi-objective particle swarm algorithm as the solution algorithm, and the simulation iterative process is completed through Python programming and the com interface of Vissim software. In order to verify the validity of the model and algorithm, the actual three-intersections arterial road network is used for verification, and the model in this study is compared with the optimization model without considering MFD, the model solved by traditional algebraic method, and the optimization model solved by typical multi-objective particle swarm. Results show that the model in this research performs well in efficiency indicators such as total delay, average delay, and queue coefficient. At the same time, the MFD form has highest stability, the control effect is the best in the saturated state. The solution algorithm GA-MOPSO also has a better solution effect.

Keywords: *multi-objective optimization, arterial coordination control, macroscopic fundamental diagram, traffic simulation*

To cite this article:

Lin, X., Lin., X, Chen, K., (2022). Saturated arterial coordinate control strategy optimization considering macroscopic fundamental diagram. Archives of Transport, 62(2), 73-90. DOI: https://doi.org/10.5604/01.3001.0015.9253

Contact:
1) Lxh2020@gdcp.edu.cn [https://orcid.org/0000-0002-6854-2178] – corresponding author; 2) gdcplxh@qq.com [https://orcid.org/0000-0002-4126-5430] 3) 925197501@qq.com [https://orcid.org/0000-0002-1089-754X]

1. Introduction

Traffic congestion has become one of the core factors restricting the further advancement of urbanization in China. Under the current conditions of limited urban space resources, improving the efficiency of road network operation through signal control strategies and management is an effective way to alleviate congestion (Guo et al., 2021). In the urban road network, the arterial road often bears most of the traffic load. How to coordinate the signal control of the arterial road has become the key to solving the problem of urban traffic congestion.

The existing arterial coordination control mainly follows two ideas: maximizing the green wave bandwidth and minimizing the delay. Morgan (1964) first proposed a two-way green wave coordinated control model, and the concept of green wave has been widely used; Little et al (1981) developed the arterial signal design optimization program MAXBAND by using the maximum green wave band phase difference optimization method, which is the algebraic method. The arterial control strategy of MULTIBAND has been used to this day, but its basic assumption is that all intersections have the same passing bandwidth; the literature (Gartner et al., 1991; Stamatiadis et al., 1996) proposes the classic MULTIBAND model, which takes into account the demand of road segments, and the bandwidth of different road segments can be different. Subsequent scholars have made a lot of improvements on the basis of the MULTIBAND model, such as canceling the symmetry constraint of the green wave band (Zhang et al., 2015; Yu et al., 2017) and inserting the superposition phase (Zhang et al., 2019). The above models are improved from the perspective of bandwidth and based on algebraic method. Another optimization idea is to minimize delays. Such models mostly improve the solution efficiency through intelligence search algorithms. Some authors (Wu et al., 2008; Binghua et al., 2016; Wang et al., 2021) took the minimum delay as the optimization goal, and the public cycle, offset, and green ratio were used as parameters, and solved it with a genetic algorithm. Guo et al. (2021) set the coordination phase according to the prediction of the arrival rate of traffic flow, aiming at the minimum total delay, and solved the problem with the chaotic particle swarm optimization algorithm. In addition, the use of advanced computer technology for arterial coordination control has also become a research focus in recent years. For example, predicting the length of the vehicle queue to adjust the signal control (Ye et al., 2015), using machine learning to train signaling schemes for different traffic states (Zheng et al., 2020).

To sum up, most of the current arterial coordinated control strategies are modeled from the ideas of delay minimization, green wave maximization, and multi-objective models, and are solved by intelligent optimization algorithms (Gao et al., 2017). However, as a regional road network, urban arterial road and their connecting roads are difficult to characterize the overall operation state of the network only from micro-aggregate indicators such as delays and stop times. The arterial road network does need to design a more macroscopic road network control strategy evaluation and program decision.

At the same time, the proposal and application of the Macroscopic Fundamental Diagram (MFD) provides a new idea and basis for understanding of the traffic flow characteristics and evolution process of the regional road network, and for the study of regional traffic control methods. MFD analyzes the road network at the macro level with road network detection data, which reflects the general functional relationship between the average flow and average density in the road network and the inherent objective law. The functional relationship only depends on the road network and control strategies and the road network itself, regardless of specific transportation needs (He et al., 2014). Godfrey (1969) first proposed physical model of MFD, but it was not until 2007 that Daganzo (2007;2011), Geroliminis (2011) and other scholars (Cassidy et al., 2018) elaborated the theoretical principle of MFD, and proposed that MFD objectively reflects the internal relationship between the operating state of the road network and the cumulative number of vehicles, MFD is also a general relationship between the weighted flow and the total traffic flow of the road network.

MFD research mainly focuses on: MFD existence and modeling, MFD influencing factors, and traffic control applications. In terms of MFD modeling research, scholars initially believed that the shape of MFD is close to a triangle. With the deepening of research, he proposed that MFD is more similar to trapezoid (Geroliminis & Daganzo, 2008). For the

acquisition and drawing of MFD, the mainstream estimation methods are loop detector detection method (Nagle et al., 2015) and floating car estimation method (Nagle et al., 2014). In recent years, there are also literatures (Lu et al., 2014; Jin et al., 2018; Lin et al., 2020; Ji et al., 2018) using data fusion technology for multi-source data modeling. Some studies (Buisson et al., 2009) have also focused on the impact of different spatial positions of data detectors on MFD.

In terms of MFD influencing factors, control strategy and traffic demand have been proved to have a great impact on the shape of MFD (Ji et al. 2010; Zhang et al., 2020). Tsubota et al. (2013) confirmed the impact of driving route selection on MFD and applied route guidance strategy. Xu et al. (2013) demonstrated through simulation experiments that road network traffic control strategies such as bus-only lanes and no-traffic measures have a greater impact on the form of MFD. Zhang et al. (2013) compared the MFD of the arterial road network under various signal control systems, and found that the distribution of vehicle demand is an important factor affecting the MFD. Compared with the traditional SCAT system, the MFD characteristics obtained by the adaptive signal control with the road network density distribution as the optimization goal are better. Hui et al. (2019) analyzed the influence of the arterial control strategy on MFD, and found that the public cycle, phase difference, and green-signal ratio are the main influencing factors, and there is an optimal public cycle to maximize the traffic efficiency of the arterial road network. Ji & Daamen (2010), Sun et al. (2020) put forward an identification method of key road segments in road network by identifying the influence of missing road segments on the shape of MFD. Zhu (2019) proposed using multiple MFD indicators under different traffic demands to rank the importance of road segments. Jianmin Xu et al. (2018) analyzed the sensitivity of the MFD curve to the proportion of large vehicles and proposed a corresponding vehicle conversion factor calculation method for different traffic conditions. Johari (2020) examines bus stop locations and MFDs and finds that remote bus stops result in better network performance—larger capacity and critical density range, and lower median average delays in vehicle traffic networks

The application of MFD focuses on road network state detection and discrimination, boundary control and so on. Ding et al. (2018) quickly discriminated the expressway network status by clustering the real-time MFD data. Chen (2019) and Ma et al. (2019) modeled the MFD with a three-segment trapezoid, and proposed evaluation methods such as road network capacity, stability, and road network efficiency. Dong et al. (2019) divided the control area for the road network on the basis of MFD, and then calculated the traffic state value of the sub-area through regression analysis for dynamic clustering and adjustment. Some scholars also take MFD as an index to test the stability of control strategy (Gayah et al., 2014) or network design (Hu et al., 2020).

Fu et al. (2020) proposed a partitioning algorithm that considers the multi-mode attributes of the road network, they proposed a three-step partitioning algorithm of initial sub-region division, sub-region merging, and sub-region boundary adjustment. Yan et al. (2020) proposed a two-layer optimization model for network boundary signal control based on MFD, with the goal of maximizing the total output vehicles and keeping the number of existing vehicles in each area optimal, and the algorithm proves to be more effective in the case of uneven traffic flow. . The main idea of boundary control is to coordinate the flow in and out at the boundary of the sub-region divided by MFD (Lin, 2014; Wang et al., 2019; Li et al., 2021).

To sum up, although MFD research is extensive, it is rarely involved in how MFD can be used as one of the optimization objectives to guide the optimization of road network signal control strategy. Based on this, starting from the characteristics of MFD, this study puts forward the macro efficiency evaluation indicator of MFD for the operation efficiency of road network, puts forward the fast modeling method of MFD under the simulation platform, and establishes the optimization model of multi-objective arterial control strategy considering MFD combined with the traditional evaluation indicators. Combined with the particle swarm optimization algorithm, the performance of the multi-objective search is further improved.

2. Construction of MFD and macro-evaluation indicator

2.1. Introduction of MFD

As the basic attribute of the road network, there is a corresponding MFD for any road network form. Taking the relationship model between the weighted

traffic flow in the road network and the weighted traffic density established by Daganzo, the typical mathematical representation of MFD is as follows.

$$\begin{cases} q^w = \dfrac{\sum_i q_i \cdot l_i}{\sum_i l_i} \\ k^w = \dfrac{\sum_i k_i \cdot l_i}{\sum_i l_i} \end{cases} \tag{1}$$

Where q_i, l_i, k_i are the traffic flow of the i road the length of the i road, and the traffic density of the i road. The MFD consists of a series of spatio-temporal scatter points. Daganzo found that the MFD pattern was closer to a trapezoid (Figure 1). In the Figure 1, the MFD shape increases with time and road network density, showing three stages of "free flow-saturated flow-supersaturated flow". In the free-flow stage, there is an obvious upward trend. At this time, the density and flow of the road network increase steadily, reaching the maximum flow of the road network $q^{\max}$. At this time, the operating efficiency of the road network reaches the highest level and can run at saturation for a period of time; As the density increases again to the inflection point k^2, the road network is overloaded, the traffic flow drops, the efficiency drops, and eventually it stagnates completely at $k^{\max}$. That is, a three-segment structure: an ascending segment, a stable segment, and a descending segment. The linear function expressions corresponding to the three segments are as Eqs. (2).

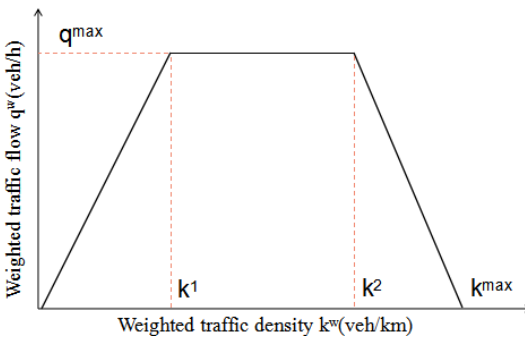

Fig. 1 Typical MFD configuration

$$q = \begin{cases} A_1 k, 0 \le k \le k^1 \\ q^{\max}, k^1 \le k \le k^2 \\ A_2 k + b, k^2 \le k \le k^{\max} \end{cases} \tag{2}$$

Compared with the use of exponential functions and multivariate functions for fitting and modeling, the three-stage MFD model has the lowest computational cost in large-scale iterative simulations, and the discrete points have less interference with the fitting results. Linear fitting results based on measured data can highly extract the main characteristics of MFD, and can also conduct intuitive and quantitative evaluation of various indicators of MFD. The data acquisition of MFD requires a large amount of detector data support, which is costly and labor-intensive, and the actual detection data integrity is limited by realistic conditions. Therefore, this study uses the micro-traffic simulation software Vissim to obtain the density and flow of each statistical interval of the road network through the acquisition of the simulated loop detector.

2.2. Macro-evaluation indicator of road network based on MFD

The traffic network is the organic unity of the travel activities of the road network. The measurement and evaluation of the operation efficiency of the road network should be able to present the traffic efficiency of traffic demand and traffic supply capacity from a macro perspective. At this stage, delays, queue lengths, and stop times are all commonly used indicators for evaluating traffic operation status. However, due to the aggregated characteristics of indicators, they are mostly used for short-term and small-scale traffic evaluation. The large-scale road network traffic evaluation cannot reflect the macro operation process and efficiency of the road network. Indicators such as average speed and total traffic flow are too macroscopic. The spatio-temporal driving characteristics of the road network are covered by a general indicator, and the differences in indicator values are small, making it difficult to judge the pros and cons of the strategy. The characteristics of MFD itself include the traffic state of the road network from free flow to saturated flow, which can just provide an effective macro evaluation of the road network. According to the characteristics of MFD, the following indicators are defined.

(1) MFD ascending segment slope: that is, the ratio

of ascending segment flow to density. Under the same road network density, the larger the road network flow, the greater the slope, which means that the overall operating efficiency of the free flow of the road network under the current control scheme is higher (Chen, 2019). The expression of the slope A_1 is as follows, k^1 is the abscissa of the inflection point of the ascending segment and the stable segment in Figure 1.

$$A_1 = \frac{q^{\max}}{k^1} \tag{3}$$

(2) Road network capacity $q^{\max}$: The existing research defines the road network capacity as the traffic flow that the road network can carry when it maintains a good operating state under certain road conditions and traffic control conditions. Existing studies have used MFD to evaluate the capacity of the road network, mostly using the density k^2 of the road network at the critical point in Figure 1 and the maximum flow $q^{\max}$ of the road network as the indicators. Considering the density k^2, it focuses on reflecting the durability of the maximum flow and the space capacity of the road network, it is difficult to directly reflect the efficiency of the road network, and it is also difficult to identify k^2 when the network conditions are not congested or not oversaturated. $q^{\max}$ reflects the maximum value of the road network traffic flow under the current control scheme, and $q^{\max}$ is more constant and easier to obtain in most network conditions, so it is defined as the road network capacity.

3. MFD modeling method based on simulation

Clustering the collected MFD data is a common method to divide the road network status (Lin et al., 2020). It is necessary to identify and divide the ascending segment, the stable segment and the descending segment in the MFD through clustering. Gaussian Mixture Model (GMM) is a model-based method, which assumes that each cluster conforms to a Gaussian linear model, and finally finds a data combination that exactly satisfies the model. where the degree to which the data belongs to the model is determined by the following probability density function (Yue et al., 2017).

$$\begin{cases} P(x) = \sum_{i=1}^{N} \phi_i p(x \mid \mu_i, \sigma_i^2) \\ = \sum_{i=1}^{N} \phi_i \frac{1}{\sqrt{2\sigma_i^2 \pi}} \exp[-\frac{(x-\mu_i)^2}{2\sigma_i^2}] \\ \sum_{i=1}^{N} \phi_i = 1 \\ 0 \le \phi_i \le 1 \end{cases} \tag{4}$$

Where N is the number of models or clusters, ϕ_i is the weight of the i model, $p(x)$ is the probability density function of the i Gaussian model, where μ_i , σ_i^2 are the corresponding mean and variance, and x is the sample data. The outstanding advantage of GMM is that it uses the attribution probability as a cluster and divides the data by ellipse, so that it has an excellent effect in clustering curve data.

For the MFD data by simulation, due to the unreasonable combination of input control parameters and uneven demand distribution, the MFD shape is often not an ideal three-segment closed trapezoidal curve, but an irregular discrete point shape. Therefore, if GMM is directly used to perform MFD three-segment clustering on the data, it will be far from the estimated contour shape, and the fitting result will lose its reference value. Therefore, it is necessary to simplify and equivalently process the MFD data and extract the key data points that can characterize the road network characteristics in the data.

The characterization of the macro-efficiency of the road network by MFD is mainly reflected in the maximum flow $q^{\max}$ of the road network in Figure 1, the slope A_1 of the ascending segment, and the slope A_2 of the descending segment. The three describe the initial operating efficiency of the road network under free flow, the upper limit of the road network capacity under saturated flow, and the anti-clogging ability under supersaturated flow. Considering that MFD will be used as one of the optimization targets later, the data points that can characterize the "upper limit" and "maximum value" of the MFD graph should be extracted first. In other words, the MFD graph should focus on preserving the upper boundary point of the trapezoidal in Figure 1. The problem is equivalent to extract the boundary points near the upper part of the dataset in the two-dimensional space. The "tic-tac-toe" boundary point ex-

traction method (Qiu et al., 2004) in image processing technology was introduced to address the issue.

The boundary points are searched and extracted in the discrete point set through the "tic-tac-toe" area in Figure 2, where the center $i(k_i, q_i)$ is the current data point, R is the radius as the search range, and the value is the average value between the points in the data set Euclidean distance, with r_1 and r_2 as the horizontal and vertical search distances, whose values are the average horizontal and vertical distances between points respectively. Then the search area around the point is divided into 8 areas. This study defines that when there are 2 continuous blank areas in the 8 areas around the point i, the point i is the boundary point. Since this method focuses on the search for the boundary points of the trapezoidal three-segment structure, the area directly below which marked with a "X" in Figure 2 is not included in the blank area search.

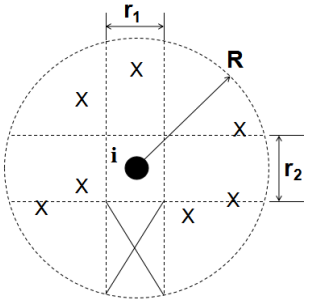

Fig. 2. "Tic-tac-toe" boundary point search scheme

$$\begin{cases} R = \dfrac{\sum_{i=1}^{N}\sqrt{(q_i - q_j)^2 + (k_i - k_j)^2}}{N} \\ r_1 = \dfrac{\sum_{i=1}^{N}\sqrt{(k_i - k_j)^2}}{N} \\ r_2 = \dfrac{\sum_{i=1}^{N}\sqrt{(q_i - q_j)^2}}{N} \end{cases} \tag{5}$$

After processing, the MFD shape with only three boundary points remaining can be obtained. The number of GMM clusters is set to 3, which corresponds to the three-segment structure in the MFD, and the linear equation system corresponding to the three-segment sample set is fitted by the least squares method. However, in practical applications, due to the inhomogeneity of road network demand in space and time, or the road network is far from supersaturated, the drawn MFD shape is often not an ideal three-segment closed trapezoid, but an unclosed one (Fig. 3 b). Approximate parabolic structure: only ascending and stable segments. Considering that this study mainly discusses the effect of MFD on the improvement of road network operation efficiency, the supersaturated congestion state corresponding to the descending segment is not considered. Therefore, the three sample sets obtained by clustering are compared. For non-closed MFD, the number of GMM clustering is changed to 2. The steps of MFD acquisition, clustering and fitting are as follows.

(1) Simulation, take k^w as the weighted traffic density and q^w as the weighted traffic flow, generate the MFD data set scatter plot, use the "tic-tac-toe" boundary search method to traverse all the data, keep only the boundary points, and obtain the preliminary MFD graph;

(2) Use GMM to cluster the obtained MFD graph, the number of clusters is 3, and obtain the sample set $U = \{U_a, U_b, U_c\}$ corresponding to the cluster;

(3) Determine the position $\{(k_a, q_a), (k_b, q_b), (k_c, q_c)\}$ of the center point of the three category sample sets of U from left to right (Figure 3), and determine the MFD shape according to the spatial position of the center point. When the MFD is satisfied $q_a < q_b$ and $q_c < q_b$, the MFD shape is a typical three-segment closed trapezoid, as shown in Figure 3(a). When the above conditions are not met, such as $q_c > q_b$, the MFD form is a non-closed parabolic structure with only an ascending segment and a stable segment, as shown in Figure 3(b), at this time, the number of clusters is changed to 2, and the GMM clustering is performed again, the data set obtained by clustering is $U = \{U_a, U_b\}$;

(4) Perform piecewise linear fitting on the final generated sample set with Eqs. (2) to obtain the final MFD graph.

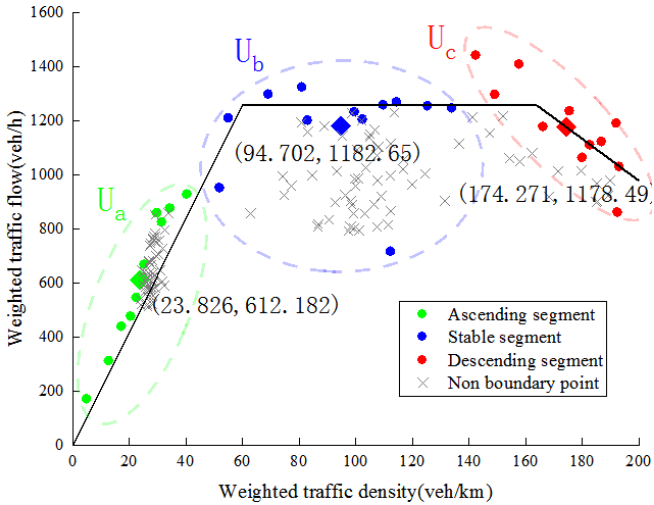

(a) Closed three-segment MFD

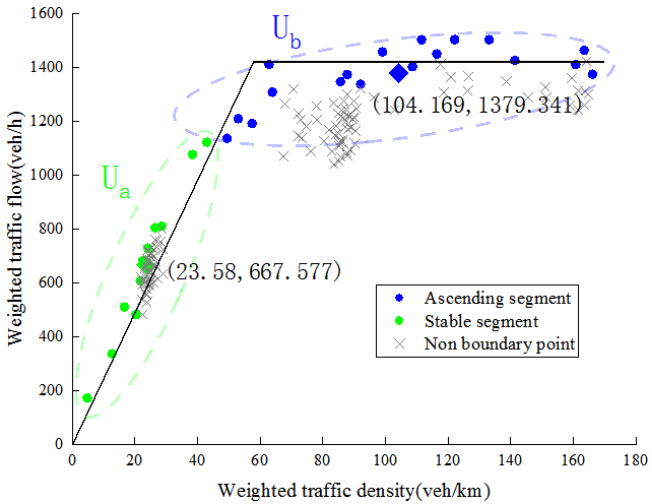

(b)non closed two-segment MFD

Fig. 3. MFD clustering and its fitting results

Using the same MFD data and comparing several MFD fitting methods (Figure. 4), it can be observed that although the curve fitted by polynomial is simple, it is difficult to define the rising slope of the curve. If GMM clustering is used directly, it is difficult to divide the trapezoidal structure, and the obtained MFD indicator also loses its representativeness. For example, the q^{max} fitting value is only 1220, which is obviously not in line with the actual MFD. If the MFD is more discrete, the above two methods The obtained indicators are even more distorted. The use of boundary point extraction and reclustering preserves the MFD features to the great extent, the trapezoidal structure can also be accurately divided, and has excellent adaptability to discrete data sets. This provides a stable foundation for subsequent iterative optimization with MFD indicators.

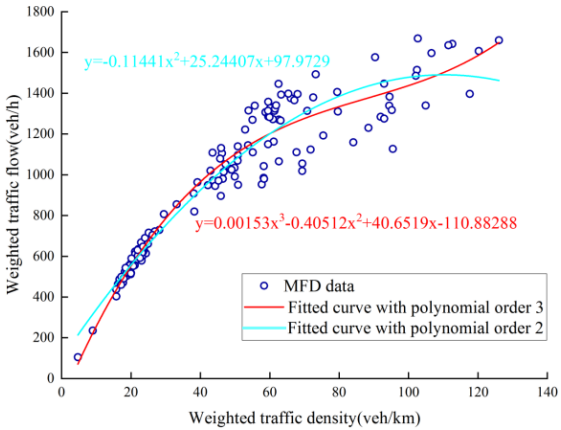

(a) fit with polynomial

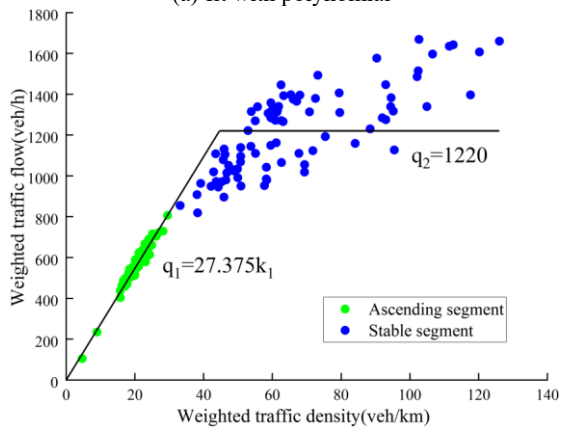

(b) GMM clustering, linear fitting

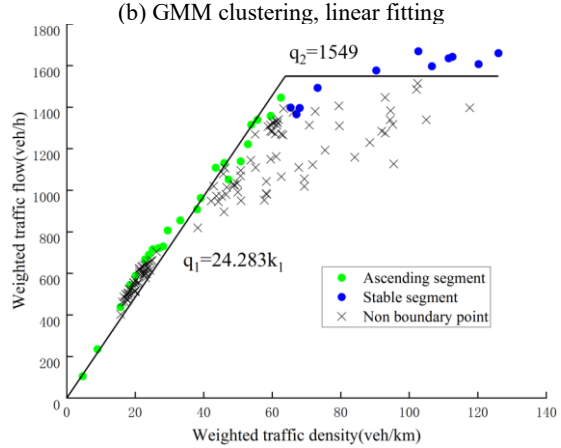

(c) "tic-tac-toe" method to extract boundary points, GMM clustering, linear fitting

Fig. 4. Various MFD fitting methods and results

4. Arterial coordination control strategy considering MFD

4.1. Multi-objective optimization model for arterial coordination

The core idea of the arterial coordination signal control strategy is to maximize the traffic efficiency of the regional road network through the design of the signal timing scheme of multiple adjacent intersections. Minimizing the average delay, queuing length, and maximizing the green wave bandwidth are common optimization goals, but such goals often make the proportion of the green light duration of the regional main road phase too large, and it is difficult to reflect the road network in long-term simulation. In order to solve the above problems, this study introduces the slope of the MFD ascending segment and the road network capacity as the macroscopic efficiency indicator of the road network to optimize and solve. The queue length is replaced by the queue coefficient, which is defined as the sum of the ratios of the queue lengths to the lane lengths for all lanes. The multi-objective optimization model of arterial coordination control considering MFD proposed in this study is shown below.

$$F(C,G,offset)=\begin{cases}\min \bar{d}\\ \min \bar{L}\\ \max q^{\max}\\ \max A_1\end{cases}$$

$$s.t.\begin{cases}\bar{L}=\sum_i^n \dfrac{queue_i}{L_i}\\ C_{\min}\le C\le C_{\max}\\ G_{i\,\min}^{j}\le G_i^j\le G_{i\,\max}^{j}\\ \sum_j G_i^j=C\\ 0\text{-}C\le offset_i\le C(i\ne 1)\end{cases} \tag{6}$$

In the Eqs. (6), $\bar{d}$ is the average control delay of vehicles in the road network output by the simulation (s); A_1 is the slope of the ascending segment of the MFD output by the simulation; the road network capacity $q^{\max}$ is obtained from the stable segment of MFD; $\bar{L}$ is the queue coefficient, which is the sum of the ratio of the average queue length of each lane to the lane length. The parameters to be solved in this study are the public cycle of each intersection, the green light time of each intersection phase, and the initial phase difference of each intersection. In the Eqs. (6), C is the public cycle (s); G_i^j is the green light time of the j phase of the i intersection (s); $offset_i$ represents the phase offset between the i intersection and the first intersection (s), and the offset of first intersection is set 0.

4.2. Multi-objective optimization algorithm based on GA-MOPSO

The objective function model in this study contains four objectives, and the objective parameters to be solved are closely related. Some indicators such as the $q^{\max}$ are difficult to determine the theoretical maximum value and cannot be normalized. Therefore, it is suitable to use non-dominated sorting and intelligent algorithm to solve.

The multi-objective particle swarm optimization (MOPSO) algorithm is a multi-objective search algorithm that combines traditional particle swarm PSO algorithm and Pareto sorting. Traditional particle swarm optimization (PSO) has particle individual optimal solution and group optimal solution. The direction and speed of particle group optimization are jointly determined by the above two parameters. MOPSO for multi-objective optimization introduces Pareto sorting on this basis, that is, the current optimal solution is determined by sorting multiple objective values through Pareto method. MOPSO has the advantages of fast convergence speed, but its disadvantages are poor population diversity and easy to fall into local optimal solutions. Genetic algorithm (GA) has remarkable effect in global search ability and population diversity, and the two algorithms complement each other (Han et al., 2021; Li et al., 2022). In this study, the multi-objective particle swarm optimization (MOPSO) is combined with the genetic algorithm (GA) operation, that is, on the basis of the MOPSO, a fast non-dominated, Pareto solution-based multi-objective with selection, crossover and mutation strategies. The optimization algorithm finally determines the most advantageous solution set in the multi-objective. The solution process is as follows (fig. 5.).

(1) Initialize the size of the particle swarm (M=15) and the initial set of parameters, that is, the public cycle, the green light time of each phase of each intersection, the offset of each intersection, and set the maximum number of iterations and

convergence conditions;

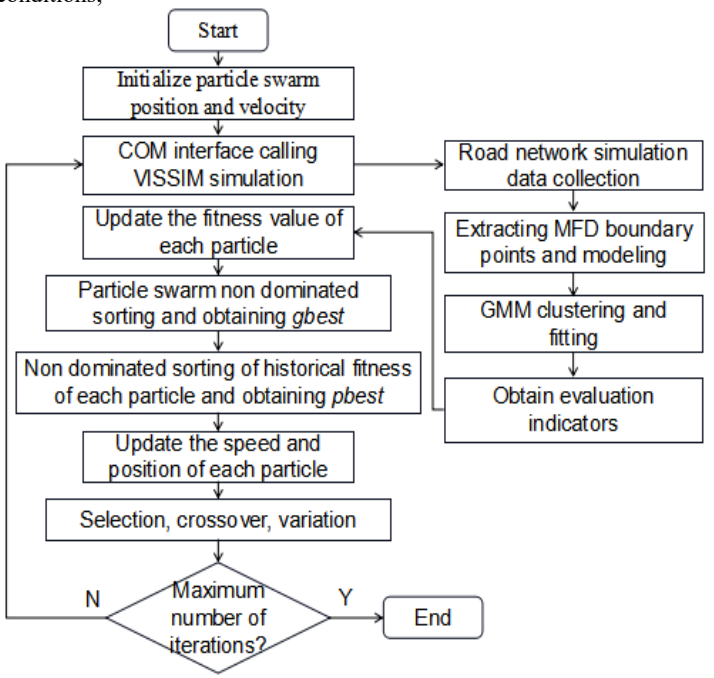

Fig. 5. GA-MOPSO multi-objective optimization framework

(2) The particle swarm changes the signal control parameters of each intersection through the com interface of Vissim for simulation, and obtains the output weighted density and weighted traffic flow of the road network. Through boundary point extracting, clustering and fitting, the slope A_1 of the MFD ascending segment and the road network capacity $q^{\max}$ of the road network are obtained. The detector obtains the average delay and queue coefficient;

(3) Perform non-dominated sorting on the historical solutions of each particle, the most advanced solution set of each particle is recorded as *pbest*, and the most advanced solution set of all particle historical sorting is recorded as *gbest*;

(4) Update the position and velocity of each particle as follows:

$$\begin{aligned} V_i &= V_i \cdot w + C \cdot r \cdot (pbest_i - x_i) + C \cdot r \cdot (gbest - x_i) \\ x_i &= x_i + V_i \end{aligned} \tag{7}$$

Where w is the inertia factor, C is the learning factor, a random number from 0 to 1, *pbest* and *gbest* are the positions with the best fitness values of the particle and the particle swarm, respectively, and they are updated in each simulation cycle;

(5) Selection operation of the genetic algorithm, select one of the particles to re-assign the parameters in the way of roulette;

(6) Crossover operation of the genetic algorithm, the algorithm choose the real number crossover method. This method refers to the combination of parameters of two chromosomes to generate two new individuals through linear combination, such as the crossover operation of the particle *am* and the particle *an* at the *j* position The method is:

$$\begin{aligned} am_j &= (1-R)am_j + Ran_j \\ an_j &= (1-R)an_j + Ram_j \end{aligned} \tag{8}$$

where R is a random number in the interval [0, 1]. Crossover between the last two chromosomes in the parent population;

(7) Mutation operation of the genetic algorithm, traverse the group of particle, and re-assign the

value randomly to the chromosome with probability P_m;

(8) Repeat steps 2-7, and check whether the constraints are satisfied in each iteration. When the convergence conditions are satisfied, the solution is ended, and the corresponding parameter value combination with the highest ranking is the best parameter combination.

5. Empirical Analysis

To verify the effectiveness of the proposed strategy and algorithm, three adjacent intersections H, I, and J of Liansheng Road in Dongguan City in China as the research object (Figure. 6). The measured traffic flow and signal phase of each intersections during 17:00-18:00 peak hours are shown in Table 1 and Figure 7.

The research uses python as the programming language, and the simulation is done using Vissim micro-simulation software. The duration of each simulation is set 9000s. In order to observe the traffic flow of the arterial road network is gradually saturated, the input traffic flow is doubled every hour. The public cycle time range is 60-200s, the cycle total loss time is 12s, the phase green light time range is 12-60s, and the road speed limit is 50km/h.

In order to verify the effectiveness of the signal control strategy, three other arterial control methods are used as comparative experiments: the method in this study is denoted as model A; Taking delay, queuing coefficient, and system traffic capacity as the objective functions, and also using GA-MOPSO to solve the coordinated control scheme, it is denoted as model B, in which the system traffic capacity is the sum of the output traffic flow at the road network intersection; the arterial coordinated control model C obtained by the traditional algebraic method; the four indicators in Eqs. (6) are used as the optimization objective, but the Model D solved by unmodified MOPSO. The characteristics of each model are shown in Table 2. Four control schemes are obtained from the solution, as shown in Table 3.

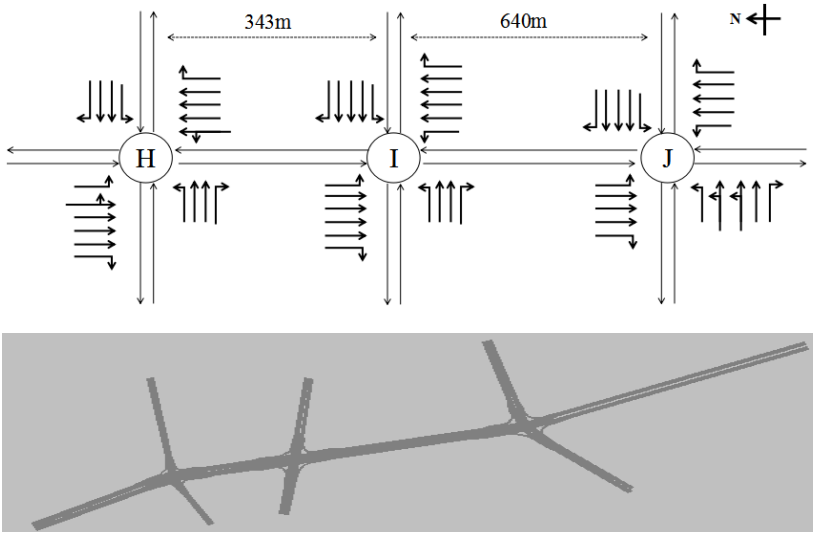

Fig. 6. Lane graph and Vissim simulation model of Liansheng Road arterial network

Table 1. Liansheng Road peak measured traffic flow(veh/h)

intersection	East			West			South			North		
	L	S	R	L	S	R	L	S	R	L	S	R
H	100	200	128	266	122	70	70	1119	100	266	1255	209
I	141	328	292	229	230	100	100	768	100	255	875	295
J	100	270	58	264	122	50	100	644	120	133	778	205

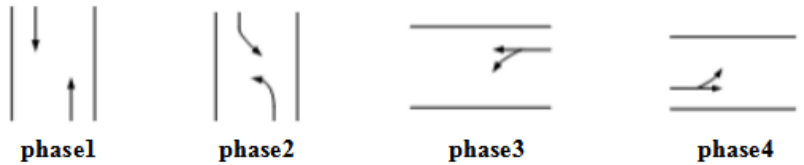

Fig. 7. Signal phase of Liansheng Road intersections (The three intersections have the same phase)

Table 2. Four optimization model features

Model	Average delay	Queuing coefficient	q^{max}	slope A_1	Road network capacity	Solving algorithm
A	√	√	√	√		GA-MOPSO
B	√	√			√	GA-MOPSO
C						Algebraic method
D	√	√	√	√		MOPSO

Table 3. Control Schemes of Four Model

Model	A			B			C			D		
Phase	H	I	J	H	I	J	H	I	J	H	I	J
1	19	15	13	25	13	26	60	51	74	32	26	33
2	12	13	15	21	21	20	51	60	38	27	20	14
3	12	13	15	12	19	12	29	27	26	22	21	25
4	12	14	12	12	17	12	25	27	27	12	26	21
Offset	0	22	27	0	52	65	0	3	46	0	11	61
Public cycle	67			82			177			105		

In order to comprehensively evaluate the advantages and disadvantages of the four models in the optimization effect, delay, queue length, MFD indicators, and system traffic capacity are used as evaluation indicators. The results are shown in Table 4 and Figure 8.

From the results, model A, that is, the multi-objective algorithm considering MFD, has the best effect in indicators such as delay and queuing coefficient. The overall MFD capacity of the road network is slightly lower than that of model B. The road network capacity under the control scheme of model A is 1664 veh/h, the slope of the MFD ascending segment is the largest, indicating that the maximum capacity is achieved the fastest among the four schemes, the low density has a higher flow rate, and the road network under free-flow state has the highest operating efficiency. However, the total delay, average delay and queuing coefficient of model B are higher than those of model A. Since the system capacity is used as the optimization target, its capacity q^{max} and system capacity indicators are slightly higher than those of model A, indicating that it has a higher output capacity in the saturated state. The evaluation indicators of model C and model D are not ideal. Model D has a better MFD indicator because it considers the MFD indicators, but it is easy to fall into the local optimal solution due to the limitation of the MOPSO algorithm. Model C prioritizes the green wave bandwidth of the main road, which leads to a large green light time, a large cycle time and huge delays on the main road.

Table 4. Effects of four model control schemes

Model	Total delay(s)	Average delay(s)	Queuing coefficient	q^{max}(veh/h)	slope A_1	System capacity(veh/h)
A	1038403	33	16.8	1664	28.661	31304
B	1145299	36	19.63	1749	26.087	31433
C	1925712	65	36.81	1621	25.408	29429
D	1273664	48	22.6	1764	26.933	30556

Model A

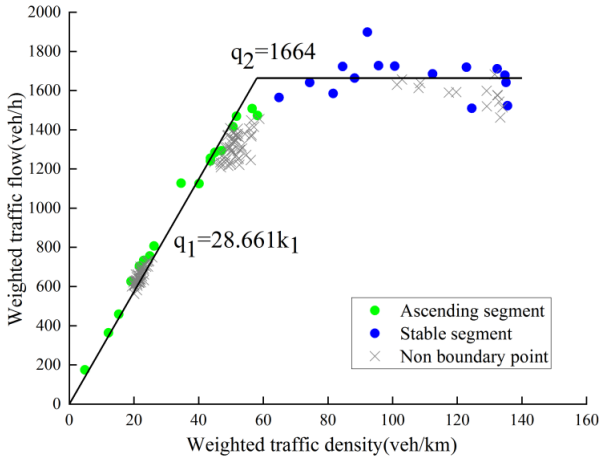

Model B

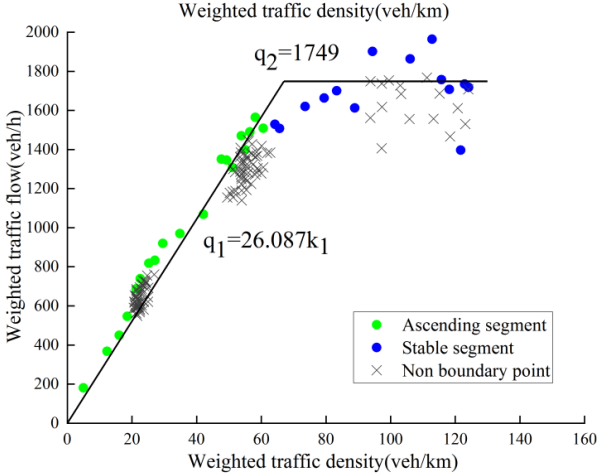

Model C

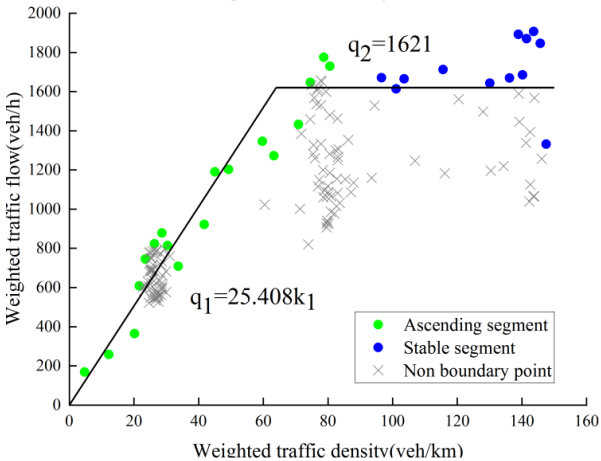

Model D

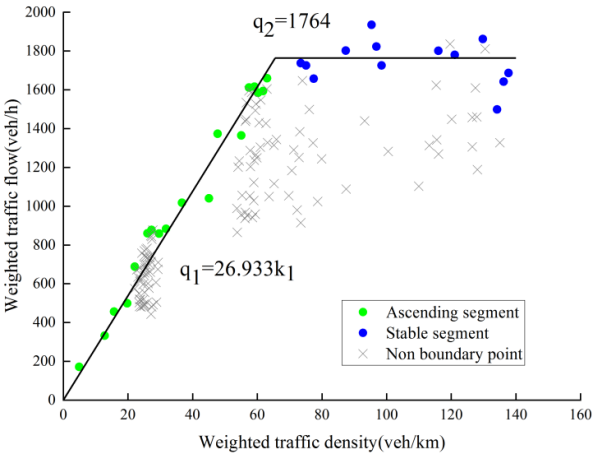

Fig. 8. MFD of four model signal control schemes

In addition, unreasonable control schemes and diversification of road conditions often make traffic distribution unbalanced, resulting in heterogeneous road network, high dispersion of MFD, and unstable state of road network. Therefore, in addition to the comparison of efficiency indicators, it is also necessary to evaluate the stability of the MFD under each scheme, and set the mean square error RMSE as the MFD stability evaluation indicator, the formula is as follows.

$$RMSE = \sqrt{\frac{\sum_{g=1}^{G}(y_g - \hat{y}_g)^2}{G}} \quad (9)$$

Where y_g is the measured value of the g statistical interval, and $\hat{y}_g$ is the fitted value. The lower the RMSE value, the better the fitting effect of the MFD, the lower the dispersion and the more stable the MFD. The fitting results and RMSE values of the above schemes are shown in Table 5 below.

Table 5. MFD stability of four model

Model	All data points: Ascending segment RMSE	All data points: Stable segment RMSE	Boundary points only: Ascending and stable segment RMSE
A	604.4	297.6	80.66
B	842.94	407.84	104.41
C	858.06	638.2	171.67
D	969.5	605.47	119.82

From the MFD form (Figure. 8) and stability results, the MFD of the four schemes are all two-segment forms that are not closed, indicating that the four schemes have not reached the state of oversaturation or congestion under the existing traffic demand and supply conditions. Among them, the corresponding scheme of model A has the largest slope A_1, from the MFD graph (Figure. 8), the data points are more concentrated, showing an obvious ascending and stable segment state, regardless of whether the non-boundary is considered or excluded. The RMSE is the smallest, the fitting effect is the best, and the MFD stability is the best; although the MFD indicators are also considered in model D, resulting in an unsatisfactory optimization effect. The discreteness is large, but the capacity q^w of the stable segment is the largest; Model C is the traditional algebraic solution method, and the public cycle value is the largest under saturated traffic flow, and the performance of each indicator is not ideal. It has higher efficiency in the free flow state of the ascending segment, but the stable segment is the most discrete under saturated flow and has the phenomenon of "back hysteresis", indicating that the traffic flow has a sudden increase or decrease under this scheme, and the road network is extremely unstable; Model B does not consider the MFD indicators, but the delay and queue length themselves are also considered indicators of traffic efficiency. Therefore, each evaluation indicator in Table 4 is close to that of model A, but its MFD stability is worse than that of model A, and the total delay is also quite different.

To sum up, the experiments show that in the scenario of arterial road network and saturated traffic flow, model A can better take into account the macro and micro traffic efficiency, the MFD form has strong stability and controllability, and the improved GA-MOPSO algorithm is far better than MOPSO, which proves the effectiveness of the model and algorithm in this study.

6. Conclusion

The macroscopic operational efficiency evaluation and optimization of the arterial road network is a necessary condition for alleviating congestion and improving regional traffic quality. In previous studies, the arterial coordinated control scheme has been proved to be a key factor affecting the form of MFD. MFD is also used to test the application effect of signal schemes.

To this end, we propose a road network performance evaluation indicator based on the characteristics of MFD and propose a method for modeling the trapezoidal structure of MFD, establish a multi-objective signal control optimization model considering the above MFD indicator, and solve it with the GA-MOPSO algorithm. The following conclusions are drawn according to the results of empirical analysis:

(1) The three-stage modeling of MFD is simple and has obvious characteristics, it can establish two macro-evaluation indicators of road network under free flow and saturated flow. In this study, boundary point extraction and GMM clustering are combined for MFD modeling. In order to avoid the interference of discrete points, and considering that the optimization goal is to pursue a greater slope of the rising section and the road network carrying capacity, the MFD boundary points tend to extract the point set above the MFD. Experiments show that this extraction and strategy can retain the key features of MFD and accurately divide two or three segments of MFD. This method is suitable for most forms of MFD.

(2) Compared with the original MOPSO, the solution algorithm using GA fused with MOPSO can jump out of the local optimum and greatly improve the solution efficiency and effect.

(3) In the saturated flow state, the multi-objective model considering the MFD indicator has an advantage in the overall control effect, and the MFD shape stability is the strongest. However, in many experiments, this optimization model A always has one or two indicators that are slightly lower than model B. The reason may be that the non-dominated sorting algorithm is not suitable for optimization of more than three objectives. On the other hand, the road network efficiency is also related to the average vehicle delay, queue length and other indicators, which makes the results of the two optimization models close.

(4) In this paper, it is feasible to use MFD and its indicators directly in signal scheme optimization modeling. In the next work, more general MFD modeling and optimization methods will be studied, and the transfer of this research method to a larger-scale road network will be explored.

Acknowledgement

This study is jointly funded by Natural Science Foundation of Guangdong Province (2020A1515010349), General Universities Scientific Research Platform and Project of the Guangdong Provincial Department of Education (2021KQNCX174; 2020GCZX017), Science and Technology Innovation Strategy Special Fund Project of Guangdong Province (pdjh2021b0781), and General Universities Key Scientific Research Platform and Project of Guangdong Province (2020GCZX017;2021KCXTD085).

References

[1] Binghua, He., Runmin, W., & Yisheng An. (2016). Arterial signal coordination control based on the proportional distribution of decoding methods of genetic algorithm. *Measurement & Control Technology, 35*(11), 5.

[2] Buisson, C., & Ladier, C. (2009). Exploring the impact of homogeneity of traffic measurements on the existence of macroscopic fundamental diagrams. *Transportation Research Record, 2124* (1), 127-136.

[3] Cassidy, M. J., Jang, K., & Daganzo, C. F. (2011). Macroscopic fundamental diagrams for freeway networks: Theory and observation. *Transportation Research Record*, *2260*(1), 8-15.

[4] Chen, W. (2019), *Urban Road Network Efficiency and Performance Evaluation Based on Macroscopic Fundamental Diagram* (doctoral dissertation, South China University of Technology)

[5] Chenyu, W., Wei, C., & Bing, L. (2021). Coordinated control method of non-public cycle arterial line period. *Journal of Northeast Forestry University, 49*(5), 6.

[6] Daganzo, C. F. (2007). Urban gridlock: Macroscopic modeling and mitigation approaches. *Transportation Research Part B: Methodological*, *41*(1), 49-62.

[7] Daganzo, C. F., Gayah, V. V., & Gonzales, E. J. (2011). Macroscopic relations of urban traffic variables: Bifurcations, multivaluedness and instability. *Transportation Research Part B: Methodological*, *45*(1), 278-288.

[8] Ding, H., Zhu, L., Jiang, C., & Zheng, X. (2018). Traffic state identification for freeway network based on MFD. *Journal of Chongqing Jiaotong University: Natural Science, 37* (12), 77-83.

[9] Dong, W., Wang, Y., & Yu, H. (2019). An identification model of critical control sub-regions based on macroscopic fundamental diagram theory. *Journal of Intelligent Transportation Systems*, *23*(5), 441-451.

[10] Fu, H., Wang, Y., & Chen, S. (2020). A partitioning algorithm of multimodal traffic networks for obtaining macroscopic fundamental diagram. *Industrial Engineering Journal, 23*(1), 1-9.

[11] Gartner, N. H., Assman, S. F., Lasaga, F., & Hou, D. L. (1991). A multi-band approach to arterial traffic signal optimization. *Transportation Research Part B: Methodological, 25*(1), 55-74.

[12] Gayah, V. V., Gao, X. S., & Nagle, A. S. (2014). On the impacts of locally adaptive signal control on urban network stability and the macroscopic fundamental diagram. *Transportation Research Part B: Methodological, 70*, 255-268.

[13] Geroliminis, N., & Daganzo, C. F. (2008). Existence of urban-scale macroscopic fundamental diagrams: some experimental findings. *Transportation Research Part B: Methodological, 42*(9), 759-770.

[14] Godfrey, J. W. (1969). The mechanism of a road network. *Traffic Engineering and Control, 11*(7), 323-327.

[15] Gonzales, E. J, Chavis, C., Li, Y., & Daganzo, C. F. (2009). Multimodal transport modeling for Nairobi, Kenya: insights and recommendations with an evidence-based model. *UC Berkeley: Center for Future Urban Transport: A Volvo Center of Excellence.*.

[16] Guo, H., Huang X., & Xu, J., et al. (2021). Arterial coordinated control method based on dynamic self-adaptive chaotic particle swarm optimization algorithm. *Chinese High Technology Letters,31*(11), 1189-1201.

[17] Han, L., Shi, X., Long, Y., & Zhai, Y. (2021). A test optimization selection method based on MOPSO-NSGA2 algorithm. *Electronics Optics & Control*, *28*(9), 89-93.

[18] He, Z., Guan, W., & Fan, L., et al. (2014). Characteristics of macroscopic fundamental diagram for Beijing Urban Ring Freeways. *Journal of Transportation Engineering and Information, 14*(2), 199-205.

[19] Hu, G., Lu, W., Wang, F., & Whalin, R. W. (2020). Macroscopic fundamental diagram based discrete transportation network design. *Journal of Advanced Transportation*, 2020, 1-13.

[20] Hui, Y., Zhao, J., & Jiang, S. (2019). Influence of Artery Coordinated Control Strategies on Macroscopic Fundamental Diagram. *Journal of Transport Information and Safety, 37*(4), 74-81.

[21] Ji, Y & Daamen, W. (2010). Analysis of urban road network traffic status and identification of critical links based on macroscopic fundamental diagram: Taking Qingdao as an example. *Journal of Shandong University of Science and Technology(Natural Science), 29*(5), 5.

[22] Ji, Y., Daamen, W., Hoogendoorn, S., Hoogendoorn-Lanser, S., & Qian, X. (2010). Investigating the shape of the macroscopic fundamental diagram using simulation data. *Transportation Research Record*, *2161*(1), 40-48.

[23] Ji, Y., Xu, M., Li, J., & Van Zuylen, H. J. (2018). Determining the macroscopic fundamental diagram from mixed and partial traffic data. *PROMET - Traffic&Transportation*, *30*(3), 267-279.

[24] Jin, S., Shen, L. X., & He, Z. B. (2018). Macroscopic fundamental diagram model of urban network based on multi-source data fusion. *Journal of Transportation Systems Engineering and Information Technology*, *18*(2), 108-115.

[25] Johari, M., Keyvan-Ekbatani, M., & Ngoduy, D. (2020). Impacts of bus stop location and berth number on urban network traffic performance. *IET Intelligent Transport Systems*, 14(12), 1546-1554.

[26] Li, H., Yue, L., Zhang, P., & Yang, L. (2022). Online learning group formation method from the perspective of multi-objective optimization. *Journal of Chinese Computer Systems*, *43*(4), 11.

[27] Li, R., & Liu, L. (2021). Cordon Pricing Scheme Based on Macroscopic Fundamental Diagram and Distance. *Journal of Highway and Transportation Research and Development (English Edition)*, 15(1), 81–88.

[28] Lin, X., Xu, J. (2020). Feedforward feedback iterative learning control method for the multilayer boundaries of oversaturated intersections based on the macroscopic fundamental diagram. *Archives of Transport*, *53*(1), 67-87.

[29] Little, J. D., Kelson, M. D., & Gartner, N. H. (1981). MAXBAND: A versatile program for setting signals on arteries and triangular networks. *Transportation Research Record, 795*, 40-46.

[30] Lu, S. F., Wang, J., Liu, G. H., & SHAO, W. (2014). Macroscopic fundamental diagram of urban road network based on traffic volume and taxi GPS data. *Journal of Highway and Transportation Research and Development*, *31*(9), 138-144.

[31] Ma, Y., Wen, S., & Jiang, Z. (2019). Sensitivity analysis of MFD of ring radial road network on signal cycle. *Journal of Transportation Systems Engineering and Information Technology, 19*(5), 78-85.

[32] Morgan, J. T., & Little, J. D. (1964). Synchronizing traffic signals for maximal bandwidth. *Operations Research*, *12*(6), 896-912.

[33] Nagle, A. S., & Gayah, V. V. (2014). Accuracy of networkwide traffic states estimated from mobile probe data. *Transportation Research Record*, *2421*(1), 1-11.

[34] Nagle, A. S., & Gayah, V. V. (2015). Comparing the use of link and probe data to inform perimeter metering control. *Transportation Research Board 94th Annual Meeting.*

[35] Qiu, Z. Y., Song, X. Y., Zhang, S. S., Zhang, D. H., & Yang, H. C. (2004). A new method for the extraction of boundary points from scattered data points. *Mechanical Science and Technology for Aerospace Engineering,23*(9),1037-1039.

[36] Stamatiadis, C., & Gartner, N. H. (1996). MULTIBAND-96: a program for variable-bandwidth progression optimization of multiarterial traffic networks. *Transportation Research Record*, *1554*(1), 9-17.

[37] Sun, Q., Zhao, S., Sun, L., & Zhang, Y. (2020). Analysis of urban road network operation state and identification of key road segments based on MFD -- a case study of Qingdao city. *Journal of Shandong University of science and technology: Natural Science Edition, 39*(5), 8

[38] Tsubota, T., Bhaskar, A., & Chung, E. (2013). Information provision and network performance represented by macroscopic fundamental diagram. *Proceedings of Transportation Research Board 92st Annual Meeting*.

[39] Wang, L., Li, M., He, Z., Zhang, L., & Li, Z. (2019). Multi-region state consistent collaborative control based on MFD in traffic network. *Journal of Transportation Systems Engineering and Information Technology, 019* (003), 81-87.

[40] Wang, P., Li, Y., Yang, D., & Yang, H. (2021). Macroscopic fundamental diagram traffic signal control model based on hierarchical control. *Journal of Computer Applications, 41*(2),571-576.

[41] Wu, E., Yang, X., Zhen, W., & Yuntao, C. (2008). Parameters co-optimization for artery coordinated control based on genetic algorithm. *Journal Of Tongji University (Natural Science), 36*(7), 921-926.

[42] Xu, F. F., & He, Z. C., & Sha, Z. R. (2013). (2013). Impacts of traffic management measures on urban network microscopic fundamental diagram. *Journal of Transportation Systems Engineering and Information Technology, 13*(2), 185-190.

[43] Yan, X., Xu, J., & Ma, Y. (2020). Bi-level optimization model of boundary signal control for the network based on macroscopic fundamental diagrams. *International Journal of Intelligent Transportation Systems Research*, *18*(1), 113-121.

[44] Ye, B. L., Wu, W., & Mao, W. (2015). A two-way arterial signal coordination method with

queueing process considered. *IEEE Transactions on Intelligent Transportation Systems*, *16*(6), 3440-3452.

[45] Yu, D. X., Tian, X. J., Yang, Z. S., Zhou, X. Y., & Cheng, Z. Y. (2017). Improved arterial coordinated signal control optimization model. *Journal of Zhejiang University (Engineering Science)*, *51*(10), 2019-2029.

[46] Yue, Z., Chen, F., Wang, Z., Huang, J., & Wang, B. (2017). Classifications of metro stations by clustering smart card data using the gaussian mixture model. *Urban Rapid Rail Transit*, *30*(2), 48-51.

[47] Zhang, C., Xie, Y., Gartner, N. H., Stamatiadis, C., & Arsava, T. (2015). AM-band: an asymmetrical multi-band model for arterial traffic signal coordination. *Transportation Research Part C: Emerging Technologies, 58*, 515-531.

[48] Zhang, L., Garoni, T. M., & de Gier, J. (2013). A comparative study of macroscopic fundamental diagrams of arterial road networks governed by adaptive traffic signal systems. *Transportation Research Part B: Methodological*, *49*, 1-23.

[49] Zhang, L., Yuan, Z., Yang, L., & Liu, Z. (2020). Recent developments in traffic flow modeling using macroscopic fundamental diagram. *Transport reviews*, 40(4), 529-550.

[50] Zhang, Y., Li, J., Li, X. & Zhou, Y. (2019). Study on green wave coordination control method based on ripple changes. *Journal of Transportation Engineering and Information, 17*(3), 10.

[51] Zheng, Y., Guo, R., Ma, D., Zhao, Z., & Li, X. (2020). A Novel Approach to Coordinating Green Wave System With Adaptation Evolutionary Strategy. *IEEE Access*, *8*, 214115-214127.

[52] Zhu, X., Guo, Y., & Yang, X. (2019). Segment importance ranking approach for traffic networks based on macroscopic fundamental diagram. *19th COTA International Conference of Transportation Professionals.*